Advanced Space Radiation Detector Technology Development

John D. Wrbanek, Susan Y. Wrbanek, Gustave C. Fralick
NASA Glenn Research Center, Cleveland, OH

Abstract

The advanced space radiation detector development team at NASA Glenn Research Center (GRC) has the goal of developing unique, more compact radiation detectors that provide improved real-time data on space radiation. The team has performed studies of different detector designs using a variety of combinations of solid-state detectors, which allow higher sensitivity to radiation in a smaller package and operate at lower voltage than traditional detectors. Integration of multiple solid-state detectors will result in an improved detector system in comparison to existing state-of-the-art instruments for the detection and monitoring of the space radiation field for deep space and aerospace applications.

Keywords: Radiation detectors; extraterrestrial radiation; solid state devices; cosmic rays; semiconductors (materials); miniaturization

Symbols and Acronyms

4π	solid angle of a sphere (sr)
β	velocity as a fraction of the speed of light
c	speed of light in a pure vacuum (≡ 299,792,458 $m \cdot s^{-1}$)
dE/dx	stopping power; quantity of LET ($keV \cdot \mu m^{-1}$)
e	elementary charge of an electron
$\delta(\beta\gamma)$	density effect correction of stopping power due to collision at high energy
γ	Lorentz Factor ($(1-\beta^2)^{-½}$)
GaN	gallium nitride
GaP	gallium phosphide
GRC	Glenn Research Center
HEO	High Earth Orbit (altitude >35,786 km)
Hg	mercury (elemental)
HZE	high energy heavy ions (High Z and Energy; Z>2, kinetic energy >35 $MeV \cdot u^{-1}$)
I	mean excitation energy of material impacted by an ion
K	stopping power scaling factor (3070.75 $MeV \cdot m^2 \cdot mol^{-1}$)
LED	Light Emitting Diode
LEO	Low Earth Orbit (altitude <2,000 km)
LET	Linear Energy Transfer
m_e	mass of an electron (0.511 MeV/c^2)
MEMS	Micro-Electro-Mechanical Systems

NASA	National Aeronautics and Space Administration
NEO	Near-Earth Objects
Si	silicon
SiC	silicon carbide
T_{max}	maximum kinetic energy that can be imparted to an electron by an impacting ion
TOF	Time Of Flight
u	unified atomic mass unit (^{12}C mass ≡ 12 u)
UV	Ultra Violet light (wavelengths between 10 nm and 400 nm)
WBG	Wide Band Gap (electron energy band gap >1.7 eV)
ω	frequency of light
ω_p	plasma frequency (~10^{16} Hz in solids)
Z	atomic number, elementary charge of a cosmic ray ion
z/a	fraction of atomic number to atomic mass of material impacted by an ion
ZnO	zinc oxide

1. Introduction

Data from new, robust compact detectors will allow improvements of existing radiation models that will impact spacecraft design and operation during planned missions. Deep space environments and outer planetary radiation belts also need improved understanding for localized time and statistical variations of steady state and "storm" conditions (ref. 1). Closer to home, cosmic radiation is a concern for aircraft crews on intercontinental flights at very high altitude (ref. 2), and is also suspected to be a driving mechanism in large-scale global cloud cover (ref. 3).

As part of the space radiation protection research effort at NASA Glenn Research Center (GRC), the advanced space radiation detector development team is advancing the technology to develop a low-power radiation detector system capable of monitoring a wide range of high energy heavy ions (HZE ions) over a spherical (4π) aspect area (ref. 4). The technology applied to this 4π HZE Detector System enables 1) improved temperature insensitivity to changes induced by transitions from sunlight into shadow (and vise-versa), 2) improved precision with lower mass, power and volume requirements, 3) improved radiation discrimination and directional sensitivity, and 4) unique monitoring of radiation environment for planetary exploration from all directions of the celestial sphere.

The realization of the detector system leverages in-house GRC expertise and facilities in 1) harsh environment thin films, 2) silicon carbide (SiC) devices and harsh environment packaging, 3) micro-optics technology, and 4) structural radiation shielding materials. Integration of all of these technologies will result in an improved detector system in comparison to existing state-of-the-art capabilities. As mission needs change, the detector technology integration can be adapted for performance and optimal scientific benefits.

2. Full-Field Space Radiation Detector System

Current radiation detector technology is limited in lifetime, precision, discrimination, and directional sensitivity for the mass, power, and volume requirements for future missions. Miniaturizing and integrating instrumentation is a high priority for addressing the challenges of manned and unmanned deep space missions to High Earth Orbit (HEO), Near Earth Objects (NEO), Lunar and Martian orbits and surfaces, and outer planetary systems, as well as for improvements to high altitude aircraft safety.

Advanced instrumentation technology for space radiation applications is specifically called for in the NASA Strategic Program Plan for Space Radiation Health Research (ref. 5). Technology requirements are defined by the National Research Council's NASA Space Technology Roadmaps and Priorities (ref. 6), the NASA Science Instruments and Sensor Capabilities Road Map (ref. 7), and the design goals of existing cosmic ray detectors (ref. 8). These requirements include particle energy range and resolution, angular coverage and resolution, and the number of sensing elements as important design criteria in trade studies.

2.1. Concept

Solutions to these challenges require the use of precision rad-hard, thermally stable detector materials and integration of a variety of detector types in a more compact, spherical geometry. Our technology approach will develop new robust, low power solid-state detectors with improved lifetime, power and noise performance. Ultimately, we will demonstrate omni-directional measurements of radiation using the integration of multiple types of detectors and materials to expand detected energy range and sensitivity for lower mass, power and volume requirements. Thus, our objective is to develop the detector technologies that will create a low-power radiation detector system capable of monitoring a wide range of HZE ions over a spherical aspect area. A design concept for the technology approach to these solutions is illustrated in Figure 1.

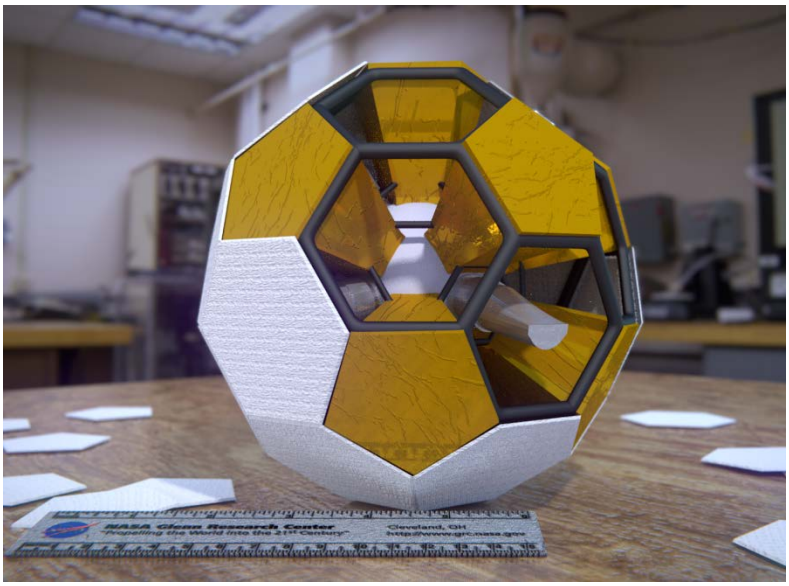

Figure 1 – Design concept illustration of a spherical space radiation detector assembly (cables and signal conditioning hardware not shown for clarity).

A variety of detector types, including low noise, wide band gap (WBG) semiconductors are considered applicable in this concept. The schematic of this spherical detector system is shown in Figure 2. The system is comprised of a central spherical Cherenkov detector surrounded by detector stacks of arrays of Linear Energy Transfer (LET) detectors as well as Triggering and Veto (rejection) detectors for signal processing.

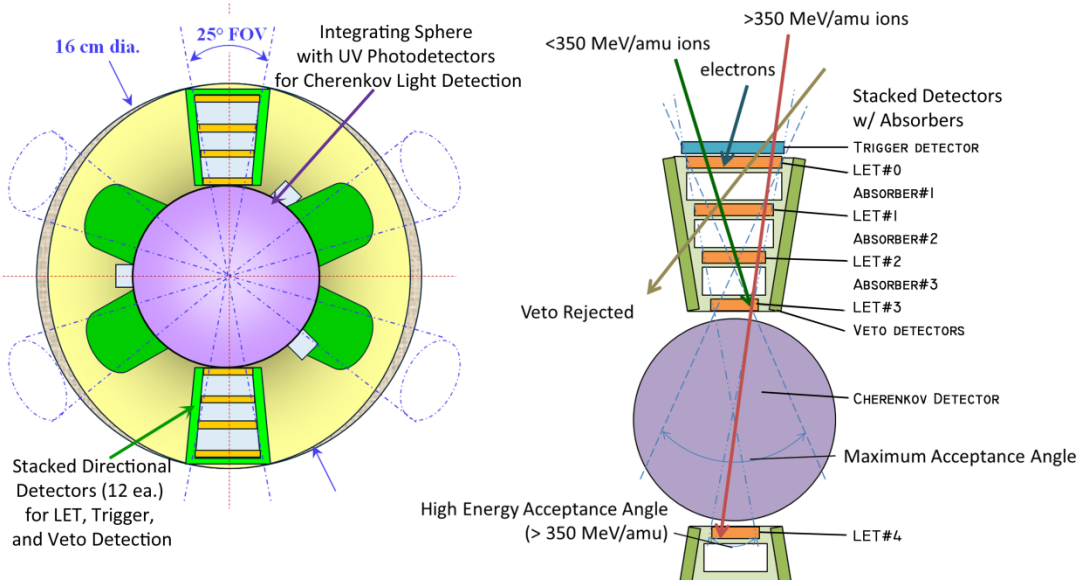

Figure 2 – Schematic drawings of concept spherical space radiation detector system showing cross section (left) and operation (right).

The technology challenge is to design and develop new detection methods in coordination with advancing these technologies. Some of the specific areas of these instrumentation efforts are:

- Solid-state detectors to use with scintillator ribbon material for Trigger and Veto detector roles over large, irregular surfaces (refs. 9, 10) where photomultiplier tube placement is not feasible. The flexibility of an advanced fiber-based detector system is an attractive option to allow embedded multidirectional radiation characterization.
- Fast solid-state spherical Cherenkov detector (ref. 11) that can detect radiation from all directions, amplifying the signal through use of integrating sphere properties designed into the detector. Current detector designs have directional sensitivity along one axis, and this spherical detector increases the directional sensitivity to multiple directions. Immersed in the space environment, where radiation is omni-directional, measurements taken over an entire spherical area at once is a significant improvement from interpolating along discrete axes.
- Stacked detector packages with various solid-state detectors, absorbers and converters for optimum detection of space radiation in a small, low-power package. A miniature detector stack will reduce mass, power, and volume requirements as well as improving particle species discrimination and spatial resolution.
- Wide band gap (WBG) solid-state devices as practical large area detectors for LET measurements. As radiation detectors, WBG semiconductors have the advantages of their low ionization energy, high electron mobility, high density and structural rigidity (ref. 12). Also, as a direct benefit for space applications, WBG semiconductors have negligible sensitivity to temperature changes.
- Reconfigurable arrangements of detector technologies to allow geometries to maximize angle coverage of cosmic radiation measurement with minimal trade-off for improved angular precision. The ability to reconfigure detector integration more easily adapts the technology to changing exploration mission needs.

Integration of all of these technologies will result in an improved detector system in comparison to existing state-of-the-art instruments. Potential improvements over the state of the art are shown the Table 1.

Table 1 - Potential improvements to critical metrics for advanced space radiation detection

Critical Metric	Current State-of-the-Art	Improvement Enablers	Proposed Detector System Performance
Energy Range	→ 140 MeV/u	Integrated Detectors	→ 1,000 MeV/u
Energy Resolution	±30 keV	Low Noise Detectors	±25 keV
Angle Coverage	0.3 cm²-sr	Spherical Geometry	1 cm²-sr
Angle Resolution	±14°	Solid-State Detectors; Spherical Geometry	±12°
Particle Species/Charge	Multiple in multiple detectors	Integrated Detectors	e → Fe
Miniaturization (Mass, Power, & Volume)	Defined by Detectors	Integrated Solid-State Detectors	30% Improvement

2.2. General Operation

The general operation of the system is conceived as initiated by the Trigger detector for a stack of directional detectors to collect the signals from LET and Cherenkov detectors in a coincidence window. If the Veto detectors are triggered during this window, the processing is halted and signal collection buffers reset. Signal processing can occur on-board after the data collection during flight or after a data download to ground operations. The LET detectors and Cherenkov detector signals are processed in parallel.

For processing, the signals from the LET detectors are fitted to a stopping power (*dE/dx*) or time-of-flight (TOF) curve, determining the charge Z and velocity β of the incoming ion based on the Bethe equation (equation 1) and an additional offset of the signal from secondary particle production (ref. 13).

$$-\left(\frac{dE}{dx}\right) = K\frac{Z^2}{\beta^2}\frac{z}{a}\left[\frac{1}{2}\ln\frac{2m_e c^2(\beta\gamma)^2 T_{max}}{I^2} - \beta^2 - \frac{\delta(\beta\gamma)}{2}\right] \quad (1)$$

Thus a minimum of three LET detectors are required for the stack, and four are planned. Electrons will be stopped in the first (outermost) LET detector of the stack, such that a bremsstrahlung/pair-production cascade effect from high energy electrons should be seen in the other LET detectors. The LET detector stack will be designed to not allow ions with energies

less than 350 MeV/u to pass through. The signals from ions greater than that energy will produce a more discernable signal in the Cherenkov detector than the LET detectors.

The Cherenkov detector returns a signal (equation 2) as a function of the incoming ion Z and β for energies greater than 340 MeV/u using an interaction sphere with an index of refraction $n(\omega)$ of 1.5 (ref. 14).

$$\left(\frac{dE}{dx}\right) = \frac{(Ze)^2}{c^2}\int_{n(\omega)>\frac{1}{\beta}}^{\omega_p} \omega\left(1 - \frac{1}{\beta^2 n(\omega)^2}\right) d\omega \qquad (2)$$

Using sapphire instead of acrylic or fused quartz lowers the minimum energy to produce a signal to 200 MeV/u. The signal from the last (innermost) LET detector of the opposite detector stack is scaled to a Z^2 value, and the β will be determined from the Cherenkov detector signal. The combination of these signals thus produces a spectrum of charge Z and kinetic energy per atomic mass from $1-(1-\beta^2)^{-½}$.

3. Detector Development

Components of this system are under development, specifically the application of WBG devices for developing the Cherenkov detector and LET measurement detectors. Potential technologies have been demonstrated for lower power, more compact detector components. Packaging options for different applications will follow once these technologies have been more clearly defined.

3.1. WBG LET Detectors

The current design of the spherical space radiation detector requires four LET detectors per stack. The largest LET detector in a stack is 450 mm² in area, with a total length of the stack to be 4.8 cm. The application of silicon carbide (SiC) in the LET detectors is based on the material's wide band gap and high displacement energy. Sensors and electronic devices made from SiC have much better resistance to radiation damage from energetic charged particles that can form defects in the semiconductor (ref. 15). The wide band gap nature of SiC also makes measurements by the detectors unaffected by thermal drift due to sun/shade transitions.

Micro-electro-mechanical-system (MEMS) based devices fabricated from silicon carbide (SiC) to conduct low-noise neutron and alpha particle spectrometry have been reported in the context of reactor core monitoring (ref. 16). A low power, low mass space radiation detector prototype system (as shown in Figure 3) using a SiC Schottky power diode (ref. 17) was developed at GRC for the NASA Exploration Technology Development and Demonstration Project for dosimetry use during future lunar missions (refs. 18, 19). The diode was selected based on the results from a study comparing the sensitivity in detecting α particles of a commercial SiC Schottky diode

and a Si PIN diode (ref. 20). The prototype system was demonstrated using a Pu-239 alpha particle source (ref. 21). Specifications for the dosimeter system are given in Table 2.

Though this prototype had one detector, the integrator can support four detectors, each with its own filter for discriminating particle type (shallow dose, deep dose, neutrons, HZE ions). For dosimetry applications, the incorporation of carbon as a significant portion of the SiC detecting medium also has the benefit of a more tissue-equivalent dose measurement over Si detectors. The approach to improve sensitivity of the dosimeter system to a broader range of space radiation in a small package was a significant improvement over the state-of-the-art radiation dosimeter devices.

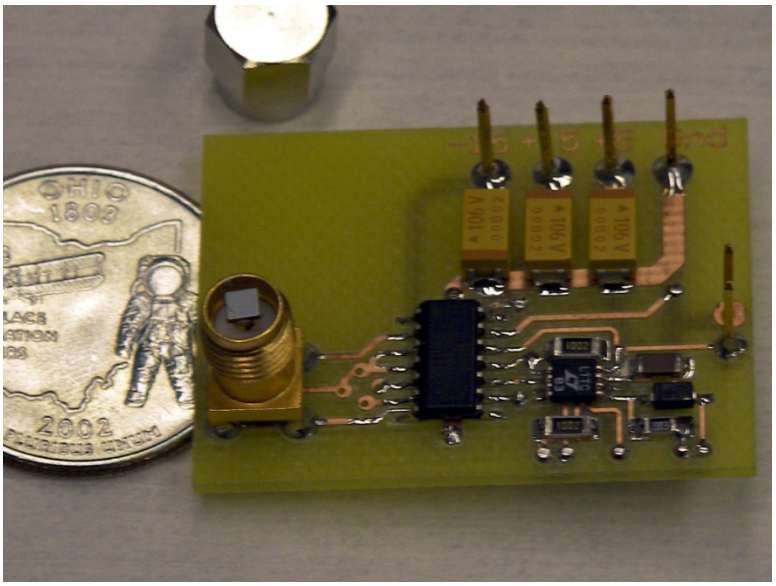

Figure 3 – SiC Dosimeter prototype developed for the NASA Exploration Technology Development and Demonstration Project

Table 2 – Low–Power SiC Dosimeter Specifications

Detector	SiC diode
Active Area	3.7 mm²
Dose Rate, max	1.27 Gy(SiC)/s (127 rad(SiC)/s)
Dose Sensitivity	1.27 mGy(SiC)/pulse (127 mrad(SiC)/pulse)
DAC	Charge Integration, 4-Channel Input, 1kHz TTL Output
Supply Voltage, max	35 V
Supply Current, max	50 mA
Weight	8 g single-channel, 30 g max
Size	4cm x 3cm x 2cm

To assemble a large area LET detector, 112 of the diodes as used in the dosimeter are needed to assemble a detector mounted in a form as seen in Figure 4. The advantages to this approach would be to allow a more direct approach of assembling the LET detectors of difference sizes without machining the semiconductor and give the option of pixel resolution in the future. As the quality of SiC crystals improve, a parallel effort will be to fabricate a large area detector from a single wafer with custom doping for specific radiation environments, with or without pixel resolution capability.

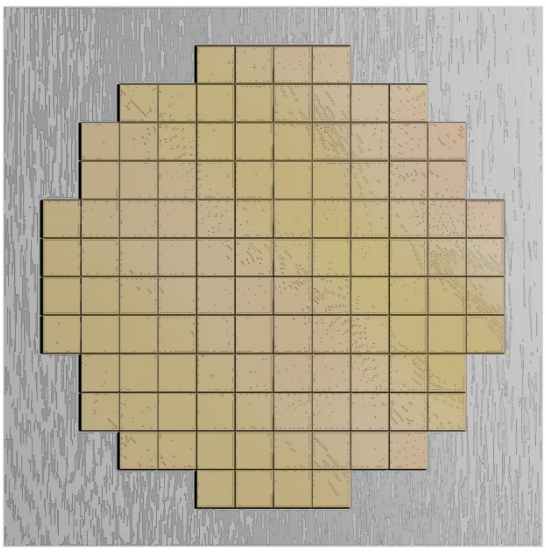

Figure 4 – Schematic for an array of 2 mm by 2 mm SiC diodes mounted in an aluminum frame to form a large area 450 mm² LET detector

3.2. Fast Solid-State Cherenkov Detector

At the heart of the spherical space radiation detector system is a spherical Cherenkov detector, 6.5 cm in diameter. Spacecraft-based radiation detector systems currently use Cherenkov detectors comprised of flat disks or blocks of sapphire or acrylic mounted on photomultiplier tubes. The goal is to replace the role of photomultiplier tubes in these types of detectors with solid-state devices, saving on size, weight and required power.

The detector will require the development of solid-state ultraviolet (UV) photo-detectors fast enough (2 ns response time or better) to detect the shockwave of Cherenkov light emitted as the ions pass through a quartz, sapphire or acrylic ball. The detector must be small enough to fit in the system structure, but have a large enough active area to capture enough Cherenkov light from the sphere for a meaningful measurement. The Cherenkov light is a broad spectrum emission proportional to the inverse square of the wavelength, peaking in the extreme UV (wavelength <150 nm), thus making lower wavelength sensitivity desirable.

Photodiodes based on wide band gap materials for detecting UV are currently limited by reaction time and/or small detector area. Commercial UV photodiodes are mainly based on three materials: gallium nitride (GaN), gallium phosphide (GaP), and silicon carbide (SiC). For all three there are tradeoffs between speed and wavelength–bandwidth sensitivity.

In the research field, UV photodetectors based on zinc oxide (ZnO) epitaxial films grown on sapphire substrates (ref. 22) and Schottky photodiodes on bulk ZnO substrates (ref. 23) have been demonstrated. With active areas less than 0.03 mm², these multi-layered devices used to investigate ZnO properties are not practical for use in Cherenkov detectors.

A fast, large area solid-state UV detector intended for application to Cherenkov detectors have been recently developed at GRC. The detector is based on the wide band gap semiconductor zinc oxide (ZnO), which in a bridge circuit can detect small, fast pulses of UV light like those required for Cherenkov detectors. A proof of concept detector was fabricated on commercially available bulk single-crystal undoped ZnO. Inter-digitated finger electrodes and contact pads were pattered via photolithography and formed by sputtered silver, as shown in Figure 5. The device tested had an electrode spacing of 20 μm and an active area of 1 mm by 2 mm (2 mm²), designed to have a 1 ns response time with 10 V applied bias voltage (ref. 11).

The ZnO-based detector was demonstrated to be sensitive to UV light at 254 nm and slightly less so at 370 nm, but not sensitive to room lighting (about 430-630 nm). Preliminary data is summarized in Table 3 that demonstrates the sensitivity of the detector to UV and compared to SiC and GaP detectors tested in parallel. These studies are preliminary, and further studies will verify the theoretical response time and general spectral sensitivity.

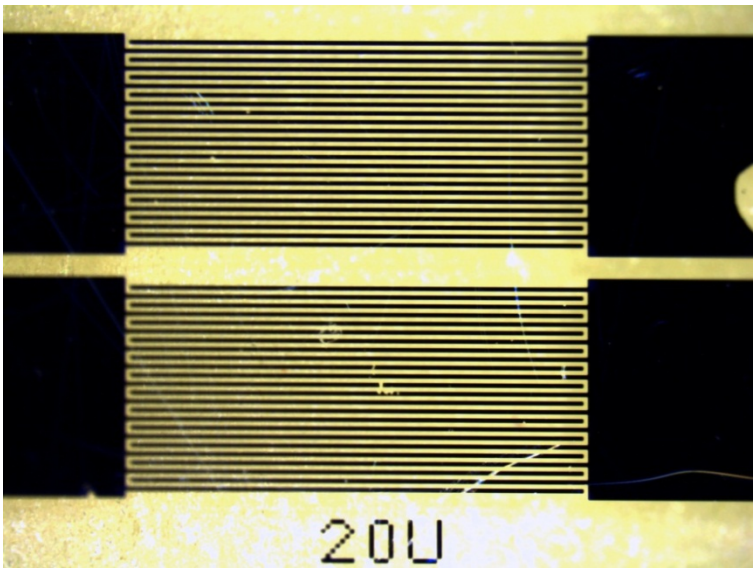

Figure 5 – Proof of concept ZnO-based UV detectors with 20 μm electrode spacing. The sizes of the inter-digitated finger areas are 1 mm by 2 mm.

This study comparing WBG UV detectors also found a potential component for the Trigger and Veto detectors, which are planned to be scintillators made of thin sheets or ribbons. The study found GaP detectors to be more sensitive to 370 nm UV source than the SiC photodiode. With emission wavelengths between 370 nm and 430 nm, scintillators are typically dependent on photomultiplier tubes for measurement and readout. The application of fast GaP photodiodes attached to fiber scintillator could be used as to minimize the size and power requirements of the Trigger and Veto detectors.

Table 3 - Relative measured sensitivity of WBG UV detectors tested

Diode	**ZnO** (per Volt bias)	**SiC** (-10V bias)	**GaP** (-10V bias)
Detector Area	2 mm²	0.96 mm²	4.8 mm²
Average Dark Current	1.8 ± 0.2 nAmps	< 50 pAmps	100 ± 20 pAmps
Relative Output to Hg lamp (254 nm)	58.7 ± 3.8	0.196 ± 0.029	1
Relative Output to LED source (370 nm)	14.99 ± 5.6	0.041 ± 0.0024	1
Relative Output to Hg lamp (254 nm) per unit area (mm^{-2})	14.09 ± 0.91	0.981 ± 0.147	1
Relative Output to LED source (370 nm) per unit area (mm^{-2})	3.6 ± 1.3	0.207 ± 0.012	1

4. Summary

To address the challenges of advancing space radiation detector technology, a low-power full-field spherical space radiation detector system is outlined. The system improves on the lifetime, precision and discrimination of radiation measurement, and allows improved performance for the mass, power, and volume requirements for future missions. The system requires technology advances to replace standard photomultiplier tubes with solid-state devices, miniaturizing detector stack geometry and improving large area detectors.

Detector development is ongoing. Investigations in WBG semiconductors have identified potential applications in Cherenkov detectors, scintillator detectors and in forming large area detectors. Demonstrations of prototype detectors based on SiC, ZnO and GaP have identified strong candidates for critical components for the advanced space radiation detector system.

Acknowledgements

The authors thank Elizabeth McQuaid and Nicholas Varaljay of the GRC Space Power & Propulsion, Communication and Instrumentation Branch for their fabrication of the ZnO UV detector discussed in this work. The authors would also like to thank Dr. LiangYu Chen of the Ohio Aerospace Institute (OAI) for his packaging of the SiC detector diode detector discussed in this work, and Joseph M. Flatico of OAI and Michael Krasowski of the GRC Optical Instrumentation and NDE Branch for designing and assembling the charge integrator for the SiC diode detector. The authors are grateful to Dr. Jon Freeman of the GRC Electron and Opto-Electronic Device Branch and Dr. Stephen P. Berkebile of the Oak Ridge Associated Universities for their respective semiconductor and shielding material studies that supported the space radiation protection effort. Finally, the authors thank Dr. Lawrence G. Matus and Roger D. Meredith of the GRC Sensors and Electronics Branch for their review and helpful comments on this text.

This work was accomplished at NASA Glenn Research Center with the support of the Space Radiation Protection Project as part of the NASA Enabling Technology Development and Demonstration (ETDD) Program, and with the support of the Center Innovation Fund as part of the NASA Space Technology Program, Office of the Chief Technologist (OCT).

References

1. Garrett, H.B., "Overview of the Jovian Environment," Presentation at the *OPFM Instrument Workshop*, June 3-5, 2008, Monrovia, California.

2. Friedberg W., Copeland K., "What Aircrews Should Know About Their Occupational Exposure to Ionizing Radiation," DOT/FAA/AM-03/16 (October 2003).
3. Perry, C.A., "Evidence for a physical linkage between galactic cosmic rays and regional climate time series," *J. Adv. Space Res*. **40** (3) (2007) 353–364.
4. Wrbanek J.D., Fralick G.C., Wrbanek S.Y., "Space radiation detector with spherical geometry," U.S. Patents 7,872,750 (January 18, 2011), 8,159,669 (April 17, 2012).
5. *Strategic Plan for Space Radiation Health Research*, Life Sciences Division, Office of Life and Microgravity Sciences and Applications (NASA 1998).
6. *NASA Space Technology Roadmaps and Priorities*, National Research Council (2012).
7. *Capability Road Map (CRM) 12: Science Instruments and Sensors (SIS) Capability Portfolio*, NASA Science Mission Directorate (2005).
8. *Managing Space Radiation Risks in the New Era of Space Exploration*, Committee on the Evaluation of Radiation Shielding for Space Exploration, National Research Council (2008).
9. Ruchti, R.C., "The Use of Scintillating Fibers for Charged-Particle Tracking," *Annu. Rev. Nucl. Part. Sci.* **46** (1996) 281–319.
10. Bross A., Crisler M., Kross B., Wrbanek J., "Scintillating fiber ribbon - tungsten calorimeter," *Nucl. Instr. and Meth. A* **286** (1-2) (1990) 69-72. FERMILAB-TM-1588 (July 1989).
11. Knoll G.F., *Radiation Detection and Measurement* (John Wiley & Sons, Inc., New York, 2000).
12. Lutz, G., "Semiconductors as Detectors," *Semiconductor Radiation Detectors: Device Physics* (Springer, Berlin, 1999).
13. Bichsel H., Groom D.E., and Klein S.R., "Passage of particles through matter," Chapter 30 in *2012 Review of Particle Physics*, Beringer J., *et al.*(PDG), PR D86, 010001 (2012).
14. Jackson J.D., *Classical Electrodynamics*, 2nd Ed. (John Wiley & Sons, Inc., New York, 1975).
15. Nava F., Bertuccio G., Cavallini A., Vittone E., "Silicon carbide and its use as a radiation detector material," *Meas. Sci. Technol.* **19** (2008) 102001.
16. Ruddy F.H., Dulloo A.R., Seidel J.G., Seshadri S., Rowland L.B., "Development of a Silicon Carbide Radiation Detector," *IEEE Trans. Nucl. Sci.* **45** (3)(1998) 536-541.
17. SiC power diode CPWR-0600-S010B 1.92 mm by 1.92 mm die, rated for 600V and 10 A maximum forward current, 600 V reverse breakdown voltage. This information is provided for identification only and does not constitute an official endorsement, either expressed or implied, by NASA.
18. Wrbanek J.D., Fralick G.C., Wrbanek S.Y., "Solid-State Personal Dosimetry," Poster presented at the *Radiation and Micrometeoroid Mitigation Technology Focus Group Meeting* Meeting, July 26-27, 2005, Hampton, Virginia. P-0875.
19. Wrbanek J.D., Fralick G.C., Wrbanek S.Y., Chen L.Y., "Active Solid State Dosimetry for Lunar EVA," *Space Resources Roundtable VII: LEAG Conference on Lunar Exploration*, LPI Contribution No. 1287 (Lunar and Planetary Institute, Houston, 2005) p. 93.

20. Wrbanek J.D., Fralick G.C., Wrbanek S.Y., Chen L.Y., "Micro-Fabricated Solid-State Radiation Detectors for Active Personal Dosimetry," NASA/TM—2007-214674 (February 2007).
21. 1.22×10^6 counts per minute, assayed July 30, 1964.
22. Liang S., Sheng H., Liu Y., Huo Z., Lu Y., Shen H., "ZnO Schottky ultraviolet photodetectors," *Journal of Crystal Growth* **225** (2001) 110–113.
23. Allen M.W., Alkaisi M.M., Durbin S.M., "Metal Schottky diodes on Zn-polar and O-polar bulk ZnO," *Applied Physics Letters* **89** (2006) 103520.